Enhancement of acoustic streaming induced flow on a focused SAW device: Implications for biosensing and microfluidics

Reetu Singh, Subramanian K.R.S. Sankaranarayanan, and Venkat R. Bhethanabotla *
Sensors Research Laboratory, Department of Chemical and Biomedical Engineering,
University of South Florida, Tampa, Florida, 33620, USA.

Abstract

Surface acoustic wave (SAW) devices used for biological species detection suffer from fouling that result from binding of non-specific protein molecules to the device surface. Non-specific binding dramatically reduces the sensitivity and selectivity of biosensors. Fluid motion induced from high intensity sound waves is called acoustic streaming. The acoustic streaming phenomenon can be used to remove these non-specifically bound proteins to allow reuse of SAW devices. Focused interdigital transducers (FIDTs) based on concentric wave surfaces can excite surface acoustic waves (SAW) with high intensity, high beam-width compression ratio and small localized area. The excited waves can be utilized to enhance the streaming induced removal of fouling proteins leading to highly sensitive biosensors.

In the present work, we have developed a 3-D FE-FSI model to investigate and analyze the streaming velocity fields and forces induced by SAW devices with focused Interdigital transducers based on concentric wave surfaces. The acoustic streaming fields and velocities are computed and analyzed. The simulated device surface displacements indicate an increased surface displacement of a focused SAW device compared to a conventional SAW device with a similar size, finger periodicity and applied input voltage. A comparison of the velocity fields between focused and conventional SAW devices indicates a significant increase in the tangential, normal, and consequently total streaming velocity as a result of focusing brought about by the FSAW devices, thereby making them more suitable for biofouling removal in biosensors compared to conventional devices.

I. Introduction

Surface acoustic wave (SAW) sensors find intensive applications in chemical and biological sensing owing to their portability, cost effectiveness, high sensitivity, and reliability [1-8]. Typically, biosensing applications require the detection and measurement of biomarkers in fluid media [9]; an example being the measurement of certain proteins in bodily fluids for the detection of ovarian cancer. The use of SAW sensors in biosensing applications requires the integration of SAW devices with microfluidics, which is the science of designing systems and processes that handle and use fluid volumes of the order of picoliters to nanoliters by reducing the dead volume in the system. In microfluidic applications, SAW devices can be used as actuators for pumping small volumes of fluid to generate high enough velocities in the small fluidic channels owing to the high intensity acoustic waves. Some applications of microfluidics include gene expression analysis using DNA chips, DNA hybridization, lab-on-chip systems, immuno-assays, micro-arrays, biosensing, drug screening, drug delivery, ultrasonic mixing, actuation, and flow cytometry to name a few [10-17]. Most of these clinical and diagnostic applications of microfluidic devices require transduction of picogram to nanogram level of biomarkers into a readable signal without interference from other proteins and biomarkers, thereby requiring high device sensitivity and selectivity. However, most of the biosensors are plagued with the issue of non-specific protein binding and therefore analyte discrimination

* Author for correspondence at email: venkat@eng.usf.edu

[18]. Thus, non-specifically bound (NSB) protein removal is a challenge in biosensing applications. Additionally, high device sensitivity is required so as to detect small enough concentrations of the analyte.

The piezoelectric crystal orientation, the Interdigital transducer (IDT) geometry/configuration, and crystal thickness determine the mode of the propagating waves. Rayleigh waves couple strongly with the fluid in contact with the sensor, launching high intensity acoustic waves into the fluid. The SAW-fluid interaction creates a pressure gradient in the direction of acoustic wave propagation in the fluid, leading to an acoustically driven streaming phenomenon known as SAW streaming [19-21] which can be used for removal of NSB proteins in order to improve sensor selectivity and sensitivity, as has been shown experimentally [22, 23]. The efficient utilization of streaming in SAW devices requires the understanding of fluid dynamics in these systems. Transducer designs that can bring about enhancement in acoustic streaming need to be identified. One such candidate is a focused SAW device, shown n Fig. 1, which can excite waves with high intensity, high beam-width compression ratio, small localized area, and high vertical displacement component [24]. This aspect of the focused SAW device can be used to increase streaming velocities and facilitate microtransport.

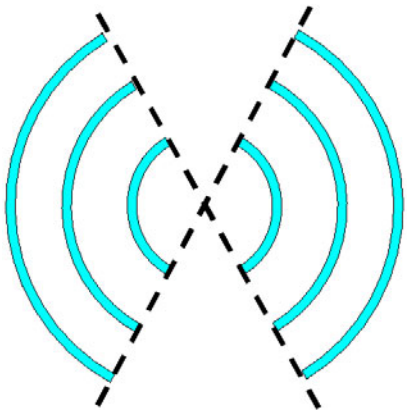

Figure 1: Schematic showing focused transducer used to enhance acoustic streaming

Structural simulations for a focused SAW device developed previously indicate increased amplitudes of surface acoustic waves in the area near the focal point, thereby making them suitable candidates for increasing the streaming capability [25]. Such models have been used in conjunction with parameters derived from the perturbation theory to predict streaming velocities and forces based on the continuum model of Nyborg [25]. However, these models ignore the effect of liquid loading and viscous dissipation in the presence of the same. The primary reason, being the simplification of the Navier-Stokes equation to ignore the viscous effects as adopted by most of the existing theories on acoustic streaming. To the best of our knowledge, there has been no three dimensional fluid structure interaction study on streaming induced by SAW devices which can quantitatively give an estimate of the streaming velocity variations introduced by viscous effects.

Understanding the interaction of the fluid field with the SAW sensor and the effects of various IDT configurations on wave propagation in the crystal requires the development of coupled field structural and FSI FE models which would enable investigation of methods to increase the acoustic streaming velocity for NSB removal while minimizing the influence of the streaming force on the sensing layer, thereby increasing the sensitivity and selectivity. The

present study represents one of the first attempts to include the effects of liquid viscosity on the streaming velocity profiles. In the present work, we have developed a 3-D FE-FSI model to investigate and analyze the streaming velocity fields and forces induced by SAW device with FIDTs based on concentric wave surfaces. The acoustic streaming enhancement brought about by the focused SAW device is analyzed by comparison with a conventional SAW device having uniform IDTs.

II. Theory

A coupled-field FSI model of a SAW device based on a micron-sized piezoelectric substrate (YZ-$LiNbO_3$) in contact with a liquid loading was developed to study surface-acoustic-wave interaction with fluid loading. A system of four coupled wave equations for the electric potential and the three component of displacement in piezoelectric materials are solved for the piezoelectric substrate or the solid domain [26]:

$$-\rho\frac{\partial^2 u_i}{\partial t^2}+c_{ijkl}^{E}\frac{\partial^2 u_k}{\partial x_j \partial x_l}+e_{kij}\frac{\partial^2 \phi}{\partial x_k \partial x_j}=0 \tag{1}$$

$$e_{ikl}\frac{\partial^2 u_k}{\partial x_i \partial x_l}-\varepsilon_{ik}^{s}\frac{\partial^2 \phi}{\partial x_i \partial x_k}=0 \tag{2}$$

These coupled wave equations can be discretized and solved for generating displacement profiles and voltages at each element/node. The piezoelectric material displacements obtained from the above equations are applied to the fluid domain at each time step.

Fluid domain was modeled using the Navier-Stokes equation; the arbitrary-Lagrangian-Eulerian approach [27] was employed to handle the mesh distortions arising from the motion of the solid substrate.

$$\rho\left(\frac{\partial v_f}{\partial t}\right)+v_f\cdot\nabla v_f+\nabla P-2\eta\nabla\cdot D=0 \tag{3}$$

$$\nabla\cdot v_f=0 \tag{4}$$

Here, v_f, P, ρ and η denote the fluid velocity, pressure, density, and viscosity, respectively. D is the rate of deformation tensor given by

$$D=\frac{1}{2}\left(\nabla v_f+(\nabla v_f)^t\right)$$

The fluid-solid coupling was established by maintaining stress and displacement continuity at the fluid-structure interface. The velocity v calculated from Eq. (3) and (4) contains harmonically varying terms and a “dc” term. The latter induces acoustic-streaming. When averaged over a relatively long time, the effect of the harmonically varying terms disappears and only the contributions from the dc part appear in the solution. The acoustic-streaming velocity ($\bar{v}_{a,i}$, i=x, y, and z) is therefore obtained by averaging v over a time period as follows:

$$\bar{v}_{a,i}=\frac{1}{T}\int_0^T v_i dt \text{ , i=}x\text{, }y\text{ and }z \tag{2.5}$$

where T is the time period of the wave propagation.

III. Computational details

A SAW device based on YZ-$LiNbO_3$ with a liquid loading was modeled to gain insights into the acoustic streaming phenomenon, using a three dimensional coupled field FSI model developed for the first time in this work. The focused SAW (F-SAW) device was constructed by adopting a pair of concentrically shaped Focused IDTs (FIDTs) (Fig 2). The dimensions of the piezoelectric substrate were 400μm width x 500μm propagation length x 200μm depth. Two IDT finger pairs in each port were defined at the surface of Y-cut, Z-propagating $LiNbO_3$ substrate. The fingers were defined with periodicity of 40 μm and the aperture width of the fingers varies depending on their radial distance from device center. The IDT fingers were modeled as mass-less conductors and represented by a set of nodes coupled by voltage degrees of freedom (DOF). The transmitting and receiving IDT's are spaced 90 microns or 2.25λ apart. The model was meshed with tetragonal solid elements with four degrees of freedom, three of them being the three translations and the fourth being the voltage. To capture the dynamics at the interface and optimize on the simulation time, the mesh was defined such that it had high density at the interface and coarser away from it. A total of 2, 218, 399 nodes and 2, 085, 877 elements were generated.

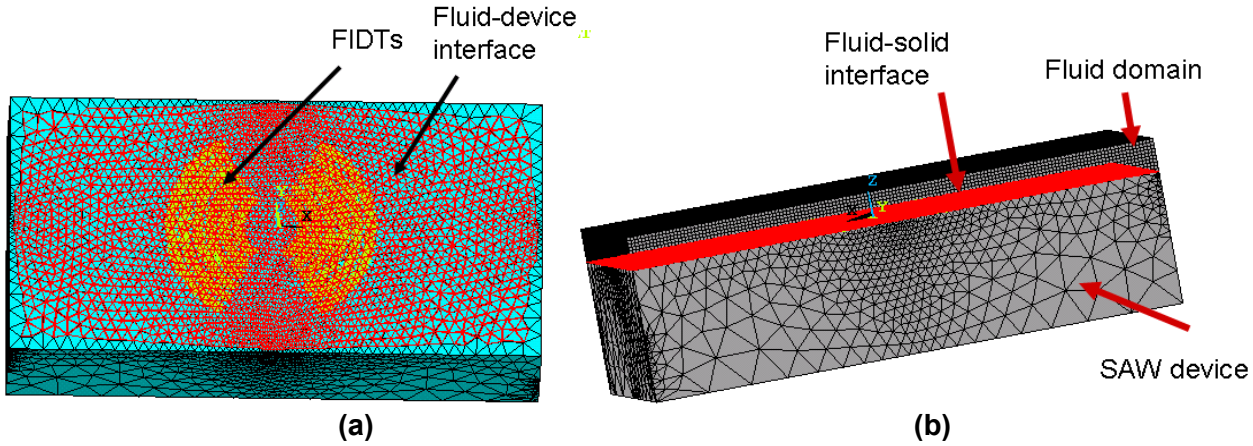

Figure 2. Focused surface acoustic wave device (a) meshed structure with FIDTs (b) with fluid loading

Fluid was modeled as incompressible, viscous, and Newtonian using the Navier-Stokes equation. In modeling fluid-solid interaction, fluid is described with reference to an Eulerian frame while the Lagrangian frame is more suited for structural/solid domain. However, the two frames are incompatible. This incompatibility is overcome by using the arbitrary Lagrangian-Eulerian (ALE) method where the mesh is constantly updated without modifying the mesh topology. In order to account for the fluid-solid interaction, an interface was defined across which displacements were transferred solid from to fluid and pressure from fluid to solid. The fluid mesh was be continuously updated as the piezoelectric substrate underwent deformation. The structure was simulated for a total of 100 nanoseconds (ns), with a time step of 1 ns. The excitation of the piezoelectric solid was provided by applying an AC voltage (with a peak value of 2.5 V and frequency of100 MHz) on the transmitter IDT fingers (Fig. 3).

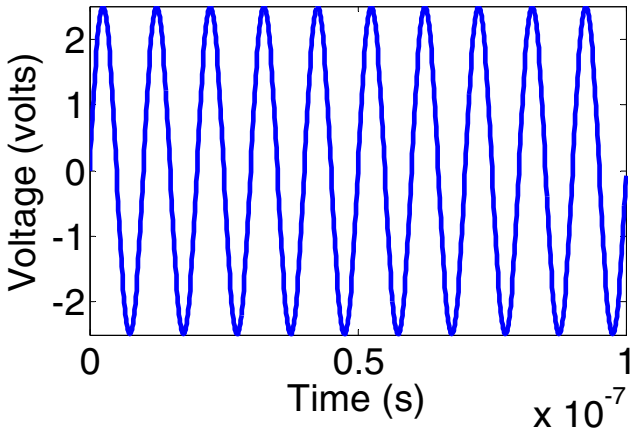

Figure 3: Applied voltage for structure excitation

IV. Results/Discussion

We have investigated wave propagation and acoustic streaming velocity fields for a focused transducer SAW device with a 120 degree arc and focal length of 85 μm, using the developed 3-D FSI model and compared them with a conventional SAW device having similar size, finger periodicity and applied input voltage to study the acoustic streaming enhancement brought about focused IDTs. Figures 4 (a, b) show the simulated device displacement contours at 70 ns, for the FSAW device as well as the conventional SAW device. Our results indicate that the maximum displacements in a FSAW device are greater than those in a conventional SAW device. In addition, the displacement field for a FSAW device tends to converge at the focal point with the maximum occurring at the focal point located at the center of the delay path and progressively decaying away from the focal point along the delay path. The acoustic energy in a FSAW device is mainly confined to the localized region near the center of the SAW delay path.

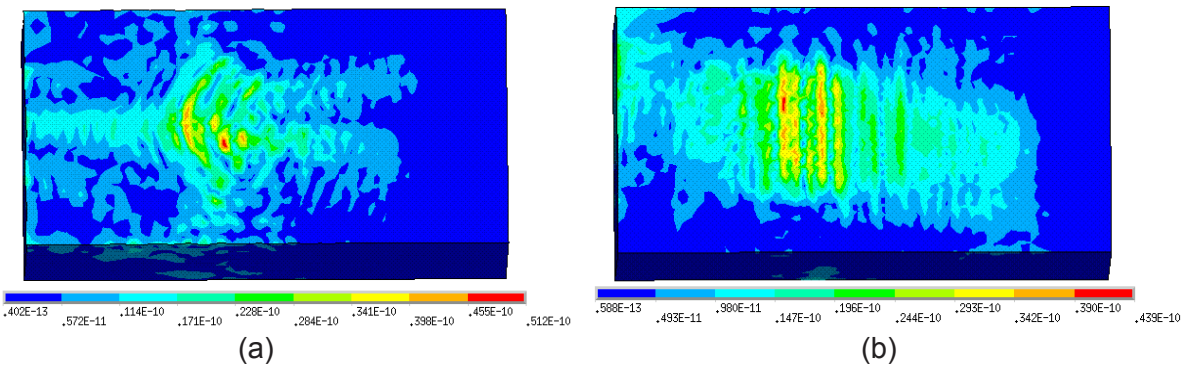

Figure 4: Contours showing the device surface displacement in response to an applied AC voltage at input IDTs at t= 70 ns for (a) FSAW device (b) conventional SAW device

Equation (5) was used to compute the streaming velocity in the F-SAW device. The calculated streaming velocity obtained for an F-SAW was compared to a conventional SAW device with the same wavelength. Figures 5(a, b) compare the tangential velocity profiles for a conventional and F-SAW device in the propagation and transverse directions; the normal and

total streaming velocity profiles are compared in Figs. 6(a, b). The velocity profiles for both the devices indicate that the highest tangential and normal velocities occur close to the device surface. The fluid motion is confined to the initial few fluid layers beyond which the wave motion is dampened significantly. In addition, beyond the first few layers, flow reversal is observed indicating fluid recirculation close to the SAW device surface. Further, the results indicate an increase in fluid velocity in both the tangential and normal directions due to the focusing effect of a FSAW device as compared to a conventional SAW device. The FSAW device brought about a 32.3% increase in total streaming velocity compared to the conventional device; the FSAW induced increase in tangential velocity was 351.8% (in direction of wave propagation) and 216.1% (in transverse direction) and the normal velocity increased by 352.7%. These results suggest that FSAW device leads to an increase in the total acoustic streaming velocity thereby leading to an increase in NSB removal efficiency, thus making the FSAW device more suited to biosensing applications.

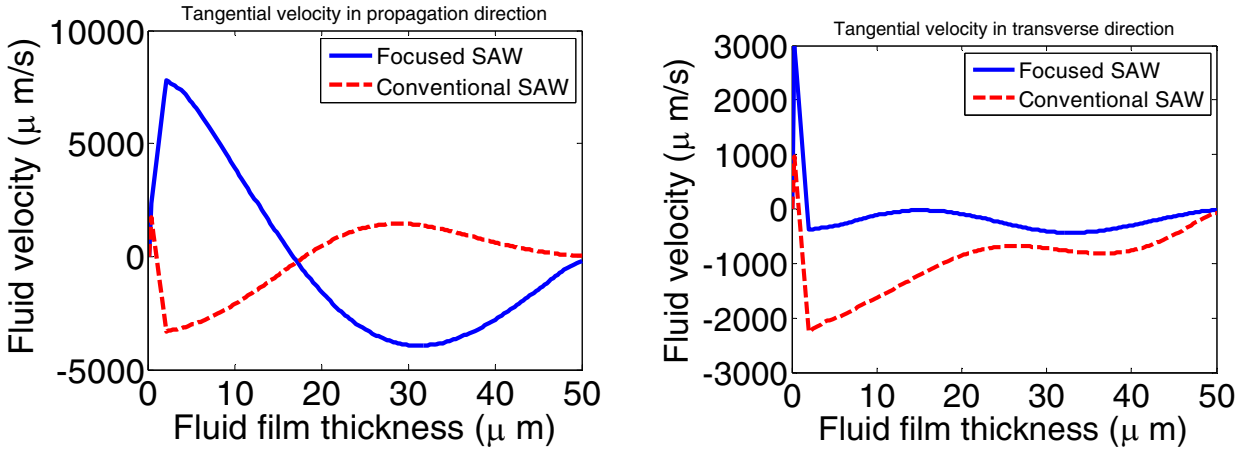

Figure 5: Comparison of tangential velocities (a) propagation direction (b) transverse direction for Focused SAW vs. Conventional SAW device for a peak input AC voltage of 2.5 V

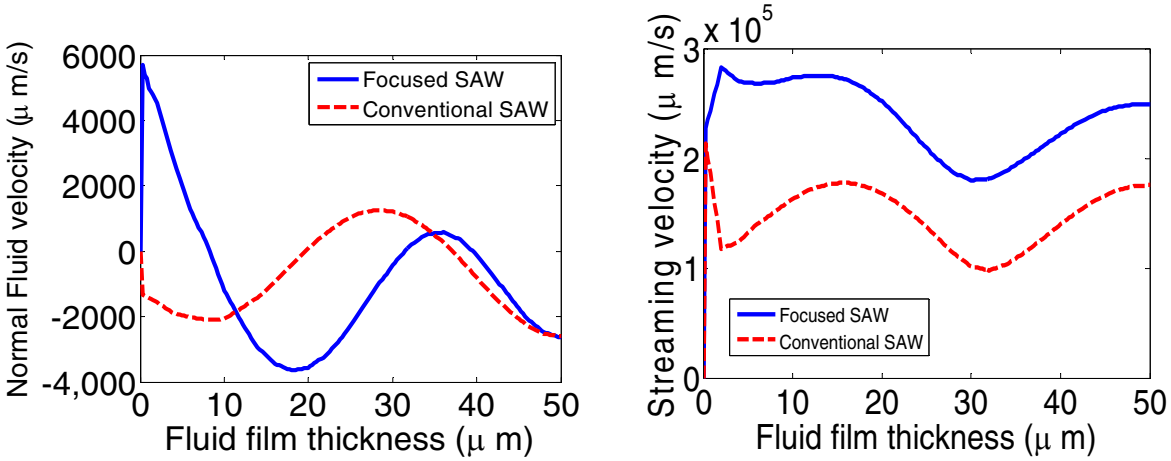

Figure 6: Comparison of (a) Normal fluid velocity (b) total streaming velocity for a Focused SAW vs. Conventional SAW device for a peak input AC voltage of 2.5 V

Conclusions

In this work, a 3D FE FSI model of an F-SAW device was developed to study the enhancement in acoustic streaming brought about by focusing. Comparison of velocity fields generated by a FSAW device, with the conventional SAW devices fabricated with uniform interdigital transducers suggests that the focused SAW devices leads to increased induced acoustic streaming velocity, thereby facilitating increased removal of non-specifically bound fouling proteins and making it more suited for biosensing applications. Further work is underway to compute and compare the streaming forces from a FSAW device with a conventional one to estimate the FSAW induced enhancement in biofouling removal.

Acknowledgements

The authors gratefully acknowledge the computational resources provided by Academic computing and Engineering computing at the University of South Florida, Tampa, FL. This work was supported by NSF grants CHE-0722887 and ECCS-0801929, and IIP-07122360.

References

1 E. Gizeli, C. R. Lowe, M. Liley, et al., Sensors and Actuators B 34, 295 (1996).

2 F. Josse, F. Bender, and R. W. Cernosek, Anal. Chem. 73, 5937 (2001).

3 Z. Li, Y. Jones, J. Hossenlopp, et al., Analytical Chemistry 77, 4595 (2005).

4 M. Hoummady, A. Campitelli, and W. Wlodarski, Smart Materials Structures 6, 647 (1997).

5 J. W. Grate, S. J. Martin, and R. M. White, Anal. Chem. 65 (1993).

6 J. W. Grate, S. J. Martin, and R. M. White, Anal. Chem. 65 (1993).

7 D. S. Ballantine and H. Wohltjen, Anal. Chem. 61, 704A (1989).

8 J. W. Grate, S. W. Wenzel, and R. M. White, Analytical Chemistry 63(15), 1552 (1991).

9 F. Josse, F. Bender, R. W. Cernosek, et al., IEEE International Frequency Control Symposium and PDA Exhibition, 454 – 461 (2001).

10 Z. Guttenberg, A. Rathgeber, S. Keller, et al., Physical Review E: Statistical, Nonlinear, and Soft Matter Physics 70, 056311/1 (2004).

11 A. G. Hadd, D. E. Raymond, J. W. Halliwell, et al., Analytical Chemistry 69, 3407 (1997).

12 A. Hatch, A. E. Kamholz, K. R. Hawkins, et al., Nature Biotechnology 19, 461 (2001).

13 K. Lange, G. Blaess, A. Voigt, et al., IEEE international ultrasonics, ferroelectrics, and frequency control joint 50th anniversary conference, 321 (2004).

14 K. Lange, F. Bender, A. Voigt, et al., Analytical Chemistry 75, 5561 (2003).

15 J. Bennès, S. Alzuaga, S. Ballandras, et al., IEEE Ultrasonics symposium, 823 (2005).

16 M. Alvarez, J. Friend, L. Yeo, et al., 16th Australian fluid mechanics conference, 621 (2007).

17 Z. H. Fan, S. Mangru, R. Granzow, et al., Analytical Chemistry 71 (1999).

18 C. M. Gregorya, J. V. Hatfielda, S. Higginsa, et al., Sensors and Actuators B: Chemical 65, 305 (2000).

19 L. Byoung-Gook, L. Dong-Ryul, and K. Kwon, Applied physics letters 89, 183505 (2006).

20 K. Chono, N. Shimuzu, Y. Matsui, et al., Japanese journal of applied physics 43, 2987 (2004).

21 K. Chono, N. Shimizu, Y. Matsui, et al., IEEE Ultrasonics Symposium 2, 1786 (2003).

22 S. Cular, D. W. Branch, V. R. Bhethanabotla, et al., AIChE Annual Meeting. (2005b).

23 S. Cular, D. W. Branch, V. R. Bhethanabotla, et al., IEEE Sensors Journal 8, 314 (2008b).

24 J. M. M. de Lima, F. Alsina, W. Seidel, et al., Journal of Applied Physics. 94, 7848 (2003).

25 S. K. R. S. Sankaranarayanan and V. R. Bhethanabolta, Journal of Applied Physics 103, 064518/1 (2008).

26 D. S. Ballantine, S. J. Martin, A. J. Ricco, et al., *Acoustic Wave sensors: Theory, design, and Physico-chemical applications* (Academic Press, San Diego, 1997)

27 J. Donea, S. Giuliani, and J. P. Halleux, Computer methods in applied mechanics. 33, 689 (1982).